Magnetic ground state of pyrochlore oxides close to metal-insulator boundary probed by muon spin rotation

M. Miyazaki,[1] R. Kadono,[1,2] K. H. Satoh,[1] M. Hiraishi,[1] S. Takeshita,[2] A. Koda,[1,2] A. Yamamoto,[3] and H. Takagi[3]
[1]*Department of Materials Structure Science, The Graduate University for Advanced Studies (Sokendai), Tsukuba, Ibaraki 305-0801, Japan*
[2]*Muon Science Laboratory and Condensed Matter Research Center, Institute of Materials Structure Science, High Energy Accelerator Research Organization (KEK), Tsukuba, Ibaraki 305-0801, Japan*
[3]*RIKEN, Wako, Saitama 351-0198, Japan*

(Received 23 June 2010; revised manuscript received 13 August 2010; published 8 September 2010)

The magnetism of ruthenium pyrochlore oxides $A_2Ru_2O_7$ (A=Hg, Cd, and Ca), whose electronic properties within a localized ion picture are characterized by nondegenerate t_{2g} orbitals (Ru^{5+},$4d^3$) and thereby subjected to geometrical frustration, has been investigated by the muon spin rotation/relaxation (μSR) technique. The A cation (mostly divalent) was varied to examine the effect of covalency (Hg>Cd>Ca) on the electronic property of the oxides. In a sample with A=Hg, which exhibits a clear metal-insulator (MI) transition below ~100 K (associated with a weak structural transition), a nearly commensurate magnetic order is observed to develop in accordance with MI transition. Meanwhile, in the case of A=Cd, where the MI transition is suppressed to the level of small anomaly in the resistivity, the local-field distribution probed by muons indicates emergence of a certain magnetic inhomogeneity below ~30 K. Moreover, in $Ca_2Ru_2O_7$, which remains metallic, highly inhomogeneous local magnetism is found below ~25 K; this magnetism arises from randomly oriented Ru moments and thus is described as a "frozen spin-liquid" state. The systematic trend of increasing randomness and itinerant character with decreasing covalency suggests a close relationship between the two characters. To understand the effect of orbital degeneracy and associated Jahn-Teller instability, we examine a tetravalent ruthenium pyrochlore, $Tl_2Ru_2O_7$ (Ru^{4+},$4d^4$). The result of μSR indicates a nonmagnetic ground state that is consistent with the formation of the Haldane chains suggested by the neutron-diffraction experiment.

DOI: 10.1103/PhysRevB.82.094413 PACS number(s): 75.25.−j, 75.47.Lx, 76.75.+i

I. INTRODUCTION

Transition-metal oxides with a chemical composition $A_2B_2O_7$ crystallize to form so-called cubic pyrochlore structures ($Fd\bar{3}m$); these structures comprise two interpenetrating networks of corner-shared tetrahedra consisting of A_2O' and B_2O_6, respectively.[1] Because of the high crystal symmetry in these crystal structures, the presence of antiferromagnetic correlation or charge disproportion between the metal ions on the pyrochlore lattice induces a geometrical frustration and associated macroscopic degrees of degeneracy for the spin/charge states within their ionic limit. This results in various interesting phenomena such as a "spin-glass" (SG) phase in $R_2Mo_2O_7$, where R=Y, Tb, and Dy (Refs. 2 and 3) and a "spin-ice" phase in $R_2Ti_2O_7$, where R=Dy and Ho (Refs. 4 and 5).

It is obviously expected that geometrical frustration (or correlation) will, in turn, have nontrivial effects on itinerant electrons, because these electrons are a local entity in a certain time scale ($\sim h/\varepsilon_t$, where ε_t is the relevant energy bandwidth). The unusual behavior of ordinary and anomalous Hall coefficients in the Mo pyrochlores with R=Nd, Sm, and Gd is probably a manifestation of such effects.[6,7] In particular, the "heavy-fermion" behavior in a metallic vanadium spinel LiV_2O_4 (in which the V ions form a pyrochlore sublattice) is one of the most interesting phenomena found in conducting pyrochlores/spinels.[8]

In the previous studies on LiV_2O_4, we demonstrated by muon spin rotation/relaxation (μSR) and muon Knight-shift measurements that unlike the local f electrons in conventional heavy-fermion metals, local vanadium moments in LiV_2O_4 are not quenched by the Kondo mechanism and that these moments induce a highly inhomogeneous and dynamically fluctuating magnetic ground state that appears to be closely related to the geometrical frustration.[9,10] Interestingly, a very similar situation was reported to occur in an intermetallic Laves phase (C15-type) compound, $Y_{1-x}Sc_xMn_2$; an earlier μSR study of this compound indicated that inhomogeneous local magnetism persists at low temperatures in a sample that exhibits a heavy-fermion behavior induced by suppression of structural phase transition (SPT) upon substitution of Y by Sc.[11] These results demonstrate urgent requirement for developing a new concept of quasiparticle state that represents the anomalous conducting state of electrons under geometrical (three-body) correlation.

From an experimental perspective, a clear understanding of anomalous metallic properties can be facilitated by determining the generic character of such electronic states by extending the μSR study to other electrically conducting pyrochlores/spinels. To this end, spinels and pyrochlores are good candidates for materials survey, although they exhibit a common tendency of undergoing structural phase transition at lower temperatures, which lifts the orbital degeneracy and relieves the frustration.

In this study, we focus on a family of ruthenium and osmium pyrochlores, $A_2B_2O_7$ (B=Ru and Os) with nominally divalent cations (i.e., $A_2^{2+}B_2^{5+}O_7$). As shown in Fig. 1, the B-site ions have a $4d^3(5d^3)$ configuration with d orbits split into e_g doublet and t_{2g} triplet states (due to the crystal fields of BO_6 octahedrons); three electrons are distributed among

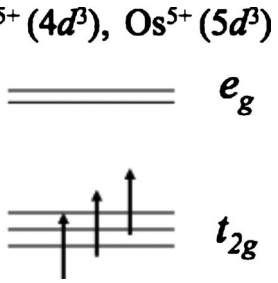

FIG. 1. Single-ion energy manifold of B site ions in $A_2^{2+}B_2^{5+}O_7$ with B=Ru and Os. Three d electrons are distributed over different t_{2g} orbitals (d_{xy}, d_{yz}, and d_{zx}), and hence, no orbital degeneracy is expected.

different t_{2g} orbits (xy, yz, zx) to satisfy both the Pauli exclusion principle and Hund coupling. Hence, there is no orbital degeneracy that might lead to the instability against the Jahn-Teller distortion and the associated structural phase transition that reduces crystal symmetry; accordingly, the effect of geometrical frustration at lower temperatures can be observed. Moreover, since the suppression of structural transition is favorable for preventing the system from undergoing metal-insulator transition (MIT), it enables the study of the effect of geometrical correlation on itinerant electrons. Interestingly, the actual ground state of these pyrochlores, as suggested from the bulk electronic properties, is found to be considerably dependent on the choice of A-site ions. As summarized in Table I, some pyrochlores exhibit MI transition that does not necessarily accompany the structural phase transition. We have shown in a recent μSR study that an osmium pyrochlore, $Cd_2Os_2O_7$, which retains its cubic structure and falls into a semi-insulating state below 225 K, exhibits a peculiar magnetic ground state which is probably related to geometrical frustration.[16] A similar but more inhomogeneous electronic state is suggested, by means of a preliminary μSR study, in the case of $Hg_2Os_2O_7$, which remains metallic down to 4 K (Ref. 15).

In this paper, we report on the magnetic ground state of ruthenium pyrochlore oxides ($A_2Ru_2O_7$) that are situated near the MI boundary. For the nominally pentavalent ruthenides ($4d^3$), the A cation ($\simeq A^{2+}$) is varied among Hg, Cd, and Ca to examine the effect of covalency (Hg>Cd>Ca) on their electronic property. In samples with A=Hg and Cd, a nearly commensurate magnetic order is observed to develop in accordance with the MI transition (below ~100 K, which is associated with weak structural transition). However, the local-field distribution at the muon site suggests the emergence of a certain magnetic inhomogeneity in $Cd_2Ru_2O_7$ below ~30 K, indicating that the spin state retains significant amount of entropy at lower temperatures. Meanwhile, in $Ca_2Ru_2O_7$ that remains metallic, a highly inhomogeneous local magnetism is observed below ~25 K; this magnetism is described by a Gaussian distribution of the local fields at the muon site, which is characteristic to the fields from randomly oriented magnetic moments situated on a regular lattice. The randomness in the magnetism is observed to increase with increasing the itinerant character of d electrons; this trend is similar to that observed in osmium pyrochlores, and it suggests a close relationship between the degree of magnetic randomness and that of delocalization. In order to understand the effect of orbital degeneracy and the associated Jahn-Teller instability, we also examine a nearly tetravalent ruthenium pyrochlore, $Tl_2Ru_2O_7$ ($Ru^{4+}, 4d^4$). The result of μSR on this pyrochlore indicates a nonmagnetic ground state that is consistent with the formation of the Haldane chains suggested by nuclear magnetic resonance (NMR) (Ref. 17) and neutron-diffraction experiments.[18,19]

TABLE I. Electronic ground state of Ru and Os pyrochlores; SPT refers to structural phase transition, indicated by x-ray diffraction data, and MIT refers to metal-insulator transition (with transition temperature T_{MI}), indicated by resistivity data. Magnetic susceptibility (χ) in $Hg_2Ru_2O_7$ and $Cd_2Ru_2O_7$ decreases sharply below T_{MI}, suggesting the development of antiferromagnetic spin correlation whereas a spin-glass (SG) -like hysteresis is observed in $Ca_2Ru_2O_7$. (The temperature dependence of χ is shown in the following sections along with the μSR result.) For the bulk properties of the Os compounds, refer to Refs. 12 and 13.

	SPT (T_s)	MIT (T_{MI})	χ drop (T_m, T_g)
$Hg_2Ru_2O_7$	≃107 K	≃107 K	≃107 K
$Cd_2Ru_2O_7$	No	No[a]	≃100 K
$Ca_2Ru_2O_7$	No	No	SG for $T_g \leq 25$ K
$Tl_2Ru_2O_7$	≃120 K	≃120 K	≃120 K
$Hg_2Os_2O_7$	No	No	≃88 K [b]
$Cd_2Os_2O_7$	No	≃230 K	≃230 K [c]

[a]Resistivity exhibits a downward kink below T_m which is followed by an upturn at lower temperatures (Ref. 14).
[b]Reference 15.
[c]Reference 16.

II. EXPERIMENT

Polycrystalline samples of $A_2Ru_2O_7$ (A=Hg, Cd, Ca, and Tl) used in this study were prepared by a solid-state reaction of AO and RuO_2 together with an oxidizer at 950 °C under a high pressure of 4 GPa. The details of the sample preparation have been described previously.[20] The bulk properties of these samples were investigated by various methods including magnetic susceptibility, electric resistivity, and specific-heat measurements. Further, structural analysis was conducted by powder x-ray diffraction technique (combined with synchrotron radiation). The result of these analyses are summarized in Table I. In order to obtain a good signal-to-noise ratio in μSR measurements, it was necessary to prepare two batches of the A=Cd, Ca, and Tl samples under the same conditions. These batches were mixed together to provide a sufficiently large sample of each compound. The susceptibility data for separate batches showed a variance of 2–3 K in the transition temperature for A=Cd and Ca and of ~5 K for A=Tl.

Among these compounds, $Hg_2Ru_2O_7$ is characterized by a sharp reduction in magnetic susceptibility (χ) below T_m ~ 107 K with a small hysteresis. This occurs in conjunction with increase in resistivity (ρ) by nearly one order of mag-

nitude and a slight lattice expansion accompanying the splitting of x-ray diffraction peaks that are attributed to simple cubic unit cell above T_m.[20] These observations led to an earlier speculation that the emergence of the spin-singlet ground state is associated with the structural phase transition. It is interesting to note at this stage that the tetravalent $Tl_2Ru_2O_7$ has many features similar to $Hg_2Ru_2O_7$: it also exhibits a sharp reduction in χ at $T_m \sim 120$ K, which is associated with the sudden increase in ρ and the structural phase transition.[18,19]

On the other hand, $Cd_2Ru_2O_7$ does not show any clear evidence of structural changes in the lattice parameters around T_m, even though it exhibits a reduction in χ below $T_m \sim 100$ K, similar to $Hg_2Ru_2O_7$. Resistivity exhibits a rather peculiar temperature dependence; it is characterized by a downward kink below T_m and, at lower temperatures, a slight upturn which suggests insulating ground state. Similar features have been reported in earlier literature.[14]

Compared with these two compounds, $Ca_2Ru_2O_7$ is more distinct in that it remains metallic at least above ~2 K. Although $\rho(T)$ shows slight enhancement at lower temperatures, it does not obey the relation $\rho(T) \propto \exp(E_a/kT)$ expected for thermally activated carriers over a band gap E_a. More interestingly, χ exhibits a cusp around $T_m \sim 25$ K, which is typically found in spin-glass systems. The present sample, which was synthesized by solid-state reaction under high pressure, exhibits features similar to those of the sample previously obtained by the hydrothermal method.[21]

Conventional μSR measurement was performed using the Lampf spectrometer installed on the M15/M20 beamlines at TRIUMF, Canada. During measurements under zero external field (ZF), the residual magnetic field at the sample position was reduced to less than 10^{-6} T while the initial muon spin direction was parallel to the muon beam direction $[\vec{P}_\mu(0) \| \hat{z}]$. For longitudinal field measurement, a magnetic field was applied parallel to $\vec{P}_\mu(0)$. Time-dependent muon polarization $[G_z(t) = \hat{z} \cdot \vec{P}_\mu(t)]$ was monitored by measuring the decay-positron asymmetry along the $\hat{z}$ axis as

$$A(t) = A_0 G_z(t) = \frac{N_+(t) - \alpha N_-(t)}{N_+(t) + \alpha N_-(t)}, \quad (1)$$

where A_0 is the initial asymmetry.

$$N_\pm(t) = N_\pm(0) e^{-t/\tau_\mu} [1 \pm A_\pm G_z(t)] \quad (2)$$

is the positron event rate for the detector placed in the forward (+) or backward (−) position relative to the sample, τ_μ is the muon decay lifetime ($=2.198 \times 10^{-6}$ s), $A_\pm$ is the decay positron asymmetry for the corresponding detector ($A_\pm \simeq A_0$), and α is the instrumental asymmetry [$\alpha = N_+(0)/N_-(0) \simeq 1$ in the usual condition]. A transverse field condition was realized by rotating the initial muon polarization so that $\vec{P}_\mu(0) \| \hat{x}$; the asymmetry was monitored along the $\hat{x}$ axis using signals from an appropriate pair of detectors for $N_\pm(t)$ to obtain $G_x(t) = \hat{x} \cdot \vec{P}_\mu(t)$.

Because of the limited quantity of samples (0.1–0.2 g) obtained by synthesis under high pressure, a special device ("muon veto counter") was installed to reduce the backgrounds due to positron events associated with muons that missed the sample. All the measurements under a magnetic field were made by cooling the sample to the target temperature after the field was equilibrated.

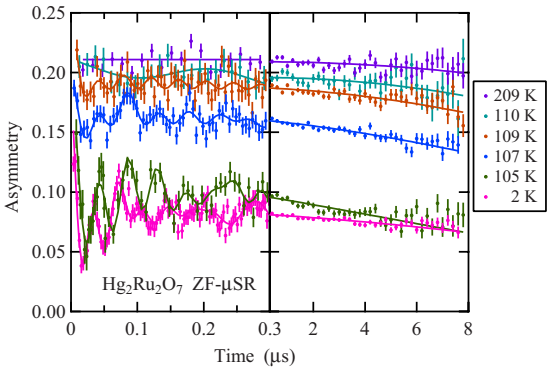

FIG. 2. (Color online) Time-dependent μ-e decay asymmetry [$A(t) \propto$ muon polarization] observed in $Hg_2Ru_2O_7$ at various temperatures under zero external field. The complete polarization ($=A_0$) corresponds to ~0.21. The development of spontaneous internal magnetic fields is inferred from the sinusoidal oscillation of $A(t)$. Solid curves are the best fits obtained using Eq. (3).

III. RESULT

A. $Hg_2Ru_2O_7$

Figure 2 shows examples of ZF-μSR time spectra over a temperature range of 2–210 K. In these spectra, an oscillatory signal is observed to emerge at around $T_m \simeq 109$ K without enhanced damping due to the critical slowdown of spin fluctuation as the temperature approaches T_m. As is also evident in the fast Fourier transform (FFT, obtained after subtracting the time-independent component) of these spectra shown in Fig. 3, the internal field shows a steplike development just below T_m, associated with a long-range magnetic order. These features are consistent with the suggestion from the hysteresis of $\chi(T)$ that the magnetic transition [which is not obvious solely from $\chi(T)$] is of the first order and occurs

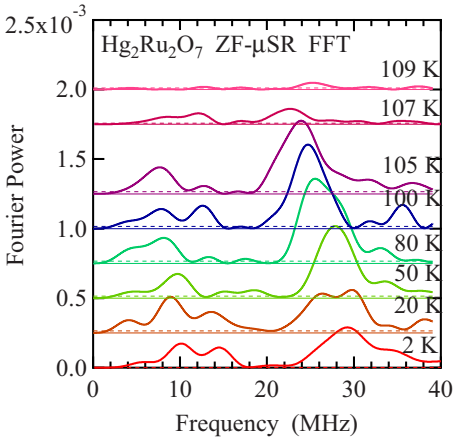

FIG. 3. (Color online) Fast Fourier transform of the μSR spectra shown in Fig. 2. Each spectrum is vertically shifted by 2.5×10^{-4} (or 5×10^{-4} between 105 and 107 K) for clarity. Dashed lines indicate the magnitude of errors for the respective spectra.

in conjunction with the structural phase transition.

The FFT spectra are characterized by two bands of dominant frequency lines around 10 and 30 MHz at 2 K, indicating the possibility of internal field distribution resulting from (i) a commensurate spin-density wave probed at a unique muon site or (ii) an antiferromagnetic state with several crystallographically nonequivalent muon sites. Considering these possibilities, we performed a curve-fitting analysis of the spectra in the time domain by means of the χ^2-minimization method using the following model function valid for the ordered phase of polycrystalline samples.

$$A(t) \simeq \sum_{i=1}^{n} A_i \left[\frac{1}{3} e^{-\lambda_L t} + \frac{2}{3} e^{-\Delta^2 t^2} e^{-\lambda_i t} \cos(2\pi f_i t + \phi) \right] + A_b, \tag{3}$$

which, in the paramagnetic phase, is reduced to

$$A(t) = (A_0 - A_b) G_z^{\mathrm{KT}}(t, \Delta) + A_b, \tag{4}$$

where $G_z^{\mathrm{KT}}(t,\Delta)$ is the Kubo-Toyabe relaxation function[22] for describing the slow Gaussian depolarization due to random local fields exerted from *nuclear* magnetic moments (with $\Delta \sim 10^{-1}$ MHz being the linewidth in the quasistatic limit); A_i, the partial asymmetry; λ_L, the longitudinal relaxation rate (which is found to be $\simeq 0$ for $Hg_2Ru_2O_7$); λ_i, the transverse relaxation rate; f_i, the muon spin precession frequency ($=\frac{1}{2\pi}\gamma_\mu B_i$ with $\gamma_\mu = 2\pi \times 135.53$ MHz/T and B_i being the local field at the muon site); ϕ, the initial phase of precession; and A_b, the background originating from muons that missed the sample ($\Sigma_i A_i + A_b = A_0$). When the dynamical fluctuation of local fields is negligible, we have

$$G_z^{\mathrm{KT}}(t,\Delta) = \frac{1}{3} + \frac{2}{3}(1 - \Delta^2 t^2) \exp\left(-\frac{1}{2}\Delta^2 t^2 \right), \tag{5}$$

$$\simeq \exp(-\Delta^2 t^2), \quad (\Delta t \ll 1) \tag{6}$$

for which the original density distribution is given by

$$P_{\mathrm{KT}}(B_\alpha, \Delta) = \frac{\gamma_\mu}{\sqrt{2\pi}} \exp\left[-\frac{\gamma_\mu^2 B_\alpha^2}{2\Delta_\alpha^2} \right] \quad (\alpha = x, y, z), \tag{7}$$

$$\Delta_x = \Delta_y = \Delta_z = \Delta, \tag{8}$$

where Δ/γ_μ denotes the root-mean-square value of the local field.

It should be noted that one third of the implanted muons is subjected to a local field parallel to their initial polarization [i.e., $\vec{P}_\mu(0) \| (B_i)_z$] in the magnetically ordered phase of polycrystalline samples. This leads to the suppression of depolarization due to nuclear random local fields for this component [$\Delta_{x,y}/\gamma_\mu \ll (B_i)_z$], as represented by the first term in Eq. (3). Meanwhile, the transverse components [the second term in Eq. (3)] are subjected to additional depolarization due to $\Delta_{x,y}$, which is approximately described by the term corresponding to Eq. (6). We adopted four components ($n=4$) which were sufficient for the satisfactory description of the entire spectra, although the spectra were found to be dominated by two of these components ($i=1$ and 3, see below).

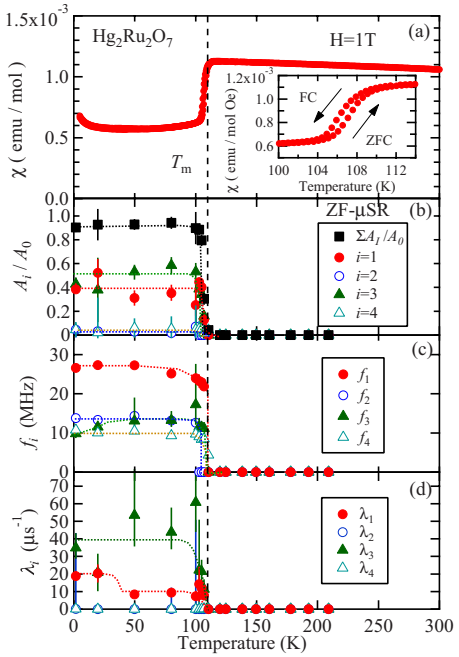

FIG. 4. (Color online) Temperature dependence of (a) bulk susceptibility and of fit parameters obtained by analysis using Eq. (3), namely, (b) fractional yield for the ordered phase defined by A_i/A_0, (c) central frequency (f_i), and (d) depolarization rate (λ_i) in $Hg_2Ru_2O_7$.

As shown in Fig. 4, the steplike development of the internal magnetic field below T_m is inferred from the temperature dependence of f_i and of the fractional yields for a magnetically ordered phase (A_i/A_0). In particular, the total fraction shown in Fig. 4(b) indicates that nearly 95% of the entire crystal is in a fully ordered state just below T_m; a small background ($A_b/A_0 \simeq 5\%$) is attributed to the presence of potassium chloride that remains as a residue of the oxidizing agent ($KClO_3$). The depolarization rate of the precession signals is relatively large for the two main components ($\lambda_i \simeq 2\pi f_i$). Moreover, while this depolarization rate is mostly independent of temperature above ~50 K, it tends to increase with decreasing temperature at lower temperatures (see λ_1); this tendency is evident from the FFT spectra. As is below, this tendency becomes very significant in the case of $Cd_2Ru_2O_7$. The low longitudinal relaxation rate (λ_L) indicates that the local field is static in the window of observation ($<10^{-1}$ MHz) and that the large value of λ_i is primarily due to the random distribution of local fields at the muon site (and not due to the dynamical fluctuation).

The Gaussian linewidth, Δ, is determined by local configuration of the nuclear magnetic moments (^{99}Ru, ^{101}Ru, ^{199}Hg, and ^{201}Hg in this case), which are the nearest-neighboring moments to the muons, and therefore, it is useful for identifying muon sites. The observed value [$\Delta \simeq 0.04(1)$ MHz] has been compared with the calculated dipole sum,

$$\Delta = \left[\frac{2}{3} \gamma_\mu^2 \sum_j \langle |\hat{\mathbf{A}}_j \boldsymbol{I}_j| \rangle^2 \right]^{1/2}, \tag{9}$$

for several possible muon sites; $\hat{\mathbf{A}}_j$ is the dipole tensor, expressed as

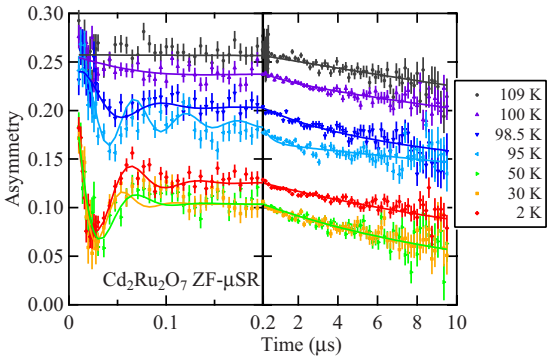

FIG. 5. (Color online) Time-dependent μ-e decay asymmetry observed in $Cd_2Ru_2O_7$ at various temperatures under zero external field ($A_0 \sim 0.25$). Solid curves are the best fits obtained using Eq. (3).

$$\hat{\mathbf{A}}_j = \frac{1}{r_j^3}\left(\frac{3\alpha_i\beta_j}{r_j^2} - \delta_{\alpha\beta}\right) \quad (\alpha,\beta = x,y,z). \tag{10}$$

The summation is done to determine the contribution of the jth nuclear magnetic moments $\boldsymbol{I}_j$ located at $\boldsymbol{r}_j=(x_j,y_j,z_j)$ from a given muon site. From the result, it is found that an interstitial position near the center of the Ru-cornered tetrahedra is the most probable site (calculated value of $\Delta = 0.04$ MHz).

The consistency of this muon site assignment with the proposed magnetic structure can be examined by comparing the magnetic fields exerted from the Ru^{5+} electronic moments

$$B_{\mathrm{loc}} = \left|\sum_j \hat{\mathbf{A}}_j \boldsymbol{\mu}_j\right| \tag{11}$$

with the internal field B_i experimentally observed ($\simeq 0.2$ T for $i=1$ and ~ 0.1 T for $i=2$ and 3); $\boldsymbol{\mu}_j$ indicates the magnetic moment of Ru ions. A recent NMR study using Hg^{199} and enriched ^{99}Ru nuclei suggests a considerably complicated magnetic structure consisting of four nonequivalent Ru sites.[23] In this study, it was considered that (i) the internal field is canceled for a quarter of Hg nuclear sites and that (ii) the angle between the primary axis of the electric field gradient and Ru magnetic moment is 90°, and hence, a magnetic multiple-$\mathbf{q}$ ($\neq \mathbf{0}$) structure was suggested, in which Ru spins are antiparallel between those mutually at the diagonal sites of Ru hexamers on the Kagomé lattice (perpendicular to the [111] axis). We additionally assume that the triangular lattice layers have an antiferromagnetic spin structure and simulate the internal field at the presumed muon site. Our simulation reproduces the two-band structure of muon precession frequency with local fields ~ 0.2 and ~ 0.4 T/μ_B. A comparison of these values with the experimental result yields the estimated Ru moment size of $\sim 0.5(1)$ μ_B, indicating the considerable reduction in the moment size from 3 μ_B.

B. $Cd_2Ru_2O_7$

The ZF-μSR spectra of $Cd_2Ru_2O_7$ (Fig. 5) are qualitatively similar to those of $Hg_2Ru_2O_7$. A signal with a spontaneous precession of muon polarization emerges below T_m

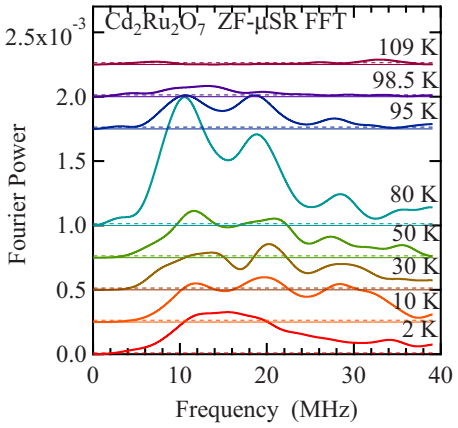

FIG. 6. (Color online) Fast Fourier transform of the μSR spectra shown in Fig. 5. Each spectrum is vertically shifted by 2.5×10^{-4} (or 7.5×10^{-4} between 80 and 95 K) for clarity. Dashed lines indicate the magnitude of errors for the respective spectra.

$\simeq 100$ K, indicating that a magnetically ordered state develops below T_m. The absence of enhancement in the relaxation rate with temperature decreasing toward T_m is a feature similar to that of $Hg_2Ru_2O_7$. From the Fourier transform of these spectra, it is found that these spectra consist of two bands of frequency lines, which are most evident around 80 K. However, such a feature, which is clearly evident over the intermediate temperature, is gradually blurred as the temperature decreases below ~ 50 K. This is clearly observed by comparing the FFT spectra of $Cd_2Ru_2O_7$ and $Hg_2Ru_2O_7$ at 2 K (Fig. 6); the former shows only a single broad band while the latter retains a two-band structure (although it also tends to broaden below ~ 50 K). Furthermore, the muon precession frequency is considerably lesser for $Cd_2Ru_2O_7$ ($\sim 12-19$ MHz) than for $Hg_2Ru_2O_7$ ($\sim 15-28$ MHz), suggesting that the corresponding effective Ru moment size is accordingly lesser.

Curve fits of these spectra in the time domain, obtained using Eq. (3), indicate that three components are required, of which one remains paramagnetic ($f_3=0$) down to 2 K (Fig. 5). The temperature dependence of fit parameters is summarized in Fig. 7. While the internal field develops sharply at temperatures lower than T_m in $Cd_2Ru_2O_7$ [as seen in Fig. 7(c)], the fractional yield of the magnetically ordered state [$(A_1+A_2)/A_0$, Fig. 7(b)] exhibits a more gradual increase with decreasing temperature than that observed in $Hg_2Ru_2O_7$ [Fig. 4(d)]. It should be noted that the variance of T_m ($\simeq 2-3$ K) due to the mixture of two-batch samples is much smaller than the change observed here. This "volumetric" development of magnetic phase suggests a tendency toward phase separation.

More interestingly, the magnetic volume fraction exhibits a decrease below $T_{m2} \sim 30-40$ K, which is associated with an increase in the fraction of the paramagnetic component (A_3). This decrease is related to enhanced depolarization of the first component ($i=1$) whose frequency merges into that of the second component ($i=2$). It is also noticeable that the bulk susceptibility exhibits a kink near T_{m2} in correspondence with the occurrence of strong depolarization. These phenomena are a clear evidence of the occurrence of a secondary magnetic phase below T_{m2}.

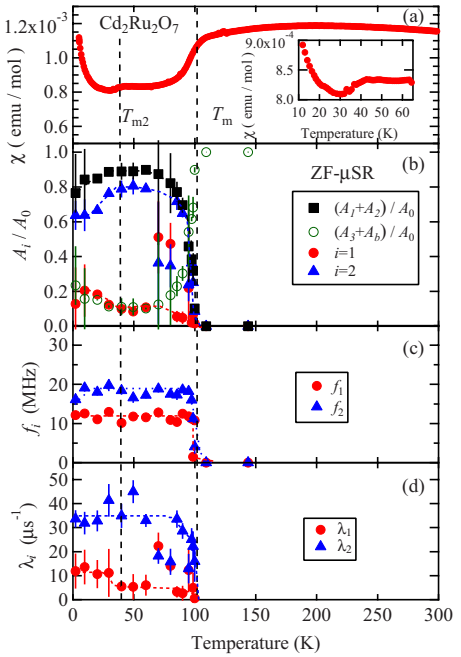

FIG. 7. (Color online) Temperature dependence of (a) bulk susceptibility (corresponding to one of the two-batch samples) and of fit parameters obtained by analysis using Eq. (3), namely, (b) fractional yield for the ordered phase defined by A_i/A_0, (c) central frequency (f_i, where $f_3=0$), and (d) depolarization rate (λ_i) in $Cd_2Ru_2O_7$.

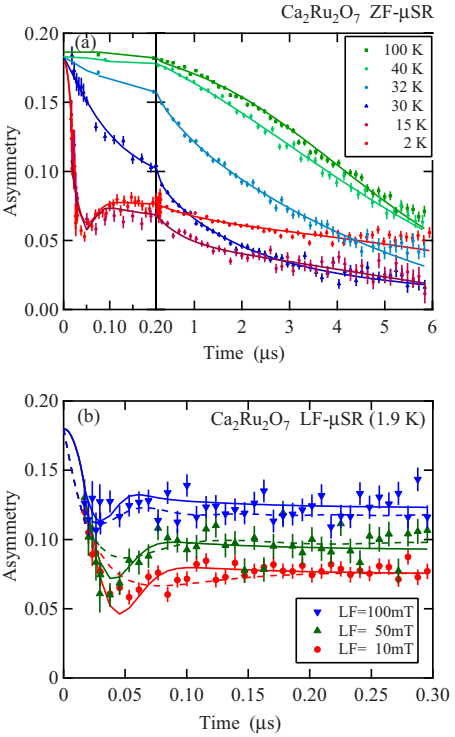

FIG. 8. (Color online) (a) Time-dependent μ-e decay asymmetry observed in $Ca_2Ru_2O_7$ at various temperatures under zero external field and (b) the initial part of the time spectra at 1.9 K under a longitudinal field of 10, 50, and 100 mT. Solid curves are the best fits obtained using Eq. (18) assuming the Gaussian distribution for the local fields (leading to the Kubo-Toyabe relaxation function) whereas dashed curves are those obtained by the Lorentzian distribution (with $\sigma=\Delta_S/\sqrt{2}$).

The low relaxation rate for the longitudinal depolarization (λ_L, not shown in Fig. 7) at 2 K indicates that the enhanced depolarization for the precession signal (λ_2) below T_{m2} arises mainly due to the enhanced quasistatic randomness of the local fields at the muon site. This has also been supported by the recovery of the asymptotic component in the μSR spectra observed under a longitudinal magnetic field. However, it should be noted that a broad peak of λ_L has been observed at around 40 K, which indicates slow residual fluctuation of local Ru moments at the intermediate temperature.

It is inferred from the value of Δ [=0.043(1) MHz which is close to that in the case of $Hg_2Ru_2O_7$] that muon sites in $Cd_2Ru_2O_7$ are common to those suggested in the case of $Hg_2Ru_2O_7$. Therefore, the observed change in the μSR spectra below T_{m2} is attributed to the change in the magnetic structure of Ru moments, which might be associated with the suppression of MI transition in $Cd_2Ru_2O_7$. Assuming that the magnetic structure of $Cd_2Ru_2O_7$ is similar to that of $Hg_2Ru_2O_7$ for $T_{m2}<T<T_m$, the reduction in the internal field at the muon site is attributed to the reduction in the effective Ru moment size to 0.36(7) μ_B, which is consistent with the enhanced itinerant feature of d electrons in $Cd_2Ru_2O_7$.

C. $Ca_2Ru_2O_7$

As mentioned earlier, the bulk property of $Ca_2Ru_2O_7$ is considerably different from that of the two previous compounds. The behavior of magnetic susceptibility in $Ca_2Ru_2O_7$ is similar to that observed in classical spin-glass systems [see Fig. 10(a)]. The ZF-μSR spectra in this compound also exhibit numerous features that are characteristic of the spin glass. As found in Fig. 8(a), these spectra exhibit an increase in depolarization rate and a corresponding change in the line shape from Gaussian to exponential-like damping as the temperature approaches the spin-glass transition temperature ($T_g \simeq 25$ K), indicating the critical slowdown of spin fluctuation toward T_g. However, a detailed analysis reveals that depolarization is not described by a simple exponential function, as in the case of a unique fluctuation rate. Moreover, the line shape below T_g (which is determined by the distribution of quasistaic local magnetic fields) is found to exhibit a distinct feature that is not observed in canonical spin-glasslike dilute alloys.

It is well known that the density distribution of the internal magnetic field (and the associated hyperfine coupling) in dilute alloys (CuMn, AuFe, etc., with Mn and Fe concentration less than 3%) is described by a Lorentzian distribution

$$P_L(B_\alpha,\sigma)=\left(\frac{\gamma_\mu}{\pi}\right)\frac{\sigma}{\sigma^2+\gamma_\mu^2 B_\alpha^2},\quad (\alpha=x,y,z) \qquad (12)$$

with σ being the factor determining the width of distribution.[24,25] This distribution is due to the strong randomness of Ruderman-Kittel-Kasuya-Yoshida (RKKY) interaction, which is effectively described by

$$s(r) \sim \frac{\cos(k_F r)}{(k_F r)^3}, \tag{13}$$

where k_F is the Fermi momentum and r is the distance between the local magnetic moments. The distance r randomly varies in the dilute limit while the interaction is long ranged (decays only by the third power of r), leading to the freezing of randomly located spins along a random orientation. The corresponding time evolution of muon polarization under zero external field has the following form.

$$G_z^L(t,\sigma) = \frac{1}{3} + \frac{2}{3}(1-\sigma t)\exp(-\sigma t), \tag{14}$$

$$\simeq \exp\left(-\frac{4}{3}\sigma t\right) \quad (\sigma t \ll 1). \tag{15}$$

Excluding the influence of spin fluctuation, the observed μSR spectra may be simply expressed as

$$A(t) = A_0 G_z^{KT}(t,\Delta) G_z^L(t,\sigma) + A_b, \tag{16}$$

which represents the line shape at the lowest temperature ($T \ll T_g$). Here, we assume that the hyperfine coupling between the electronic spins of Ru atoms and the nuclear spins are sufficiently small for the spin dynamics of the latter to be independent of the former; further, we assume that the nuclear spins remain quasistatic within the time window of μSR. This allows us to assume that muon depolarization is described by a product of the Kubo-Toyabe function (nuclear-spin part) and exponential decay (electronic part); this assumption is also made implicitly for Eq. (3). However, as shown in Fig. 8(b), the comparison of Eq. (16) with the actual spectra observed at 1.9 K indicates that this form does not reproduce the data. More interestingly, the line shape at 1.9 K is excellently described by the Kubo-Toyabe function with the linewidth replaced with that for electronic moments,

$$\Delta_S = \left[\frac{2}{3}\gamma_\mu^2 \sum_j \langle |\hat{\mathbf{A}}_j \boldsymbol{\mu}_j|\rangle^2\right]^{1/2}, \tag{17}$$

where $\Delta_S \gg \Delta$ as $|\boldsymbol{\mu}_j| \gg |\boldsymbol{I}_j|$. The comparison in Fig. 8(b) is made for a set of spectra with different external longitudinal fields (H_0) to enhance the asymptotic component in Eq. (14). These curves can be numerically obtained by replacing B_z in Eq. (12) with $B_z - \mu_0 H_0$; the same is true for Eqs. (5) and (7), where Δ is replaced by Δ_S. The response of the asymptotic component, particularly the dip around $t \simeq 0.02-0.04$ μs and quick recovery to the asymptotic value, indicates that the line shape is described by quasistatic local fields that obey Gaussian distribution.

In the detailed analysis, the observed spectra are reasonably reproduced only when we assume multiple components with different fluctuation rates of local fields. Hence, Eq. (16) should eventually be replaced with

$$A(t) \simeq G_z^{KT}(t,\Delta) \sum_{i=1}^{n} A_i G_z^{KT}(t,\Delta_S,\nu_i) + A_b, \tag{18}$$

where $G_z^{KT}(t,\Delta_S,\nu)$ is numerically obtained by solving an integral equation for the "strong collision" model,[22,26]

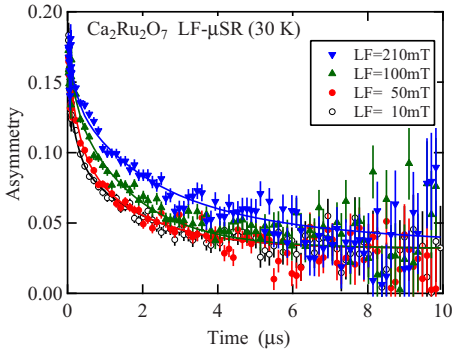

FIG. 9. (Color online) Time-dependent μ-e decay asymmetry observed in $Ca_2Ru_2O_7$ at 30 K under a longitudinal field of 10, 50, 100, and 210 mT. Solid curves are the best fits obtained using Eq. (18) assuming three components.

$$G_z^{KT}(t,\Delta_S,\nu) = G_z^{KT}(t,\Delta_S)e^{-\nu t} + \nu \int_0^t e^{-\nu\tau} G_z^{KT}(\tau,\Delta_S) G_z^{KT}(t-\tau,\Delta_S,\nu) d\tau, \tag{19}$$

which is deduced from the assumption that spin-spin correlation is described by

$$\frac{\hat{s}(0)\cdot\hat{s}(t)}{|\hat{s}(0)|^2} = e^{-\nu t}. \tag{20}$$

The best fits are obtained with two components [$n=2$ in Eq. (18)] for the spectra below T_g with Gaussian width $\Delta_S = 38.5(7)$ MHz (as found in Fig. 8, the asymptotic component exhibits a slow depolarization corresponding to $\nu_2 = 2.3(8)\times 10^8$ s^{-1} while $\nu_1 < 10^5$ s^{-1} at 1.9 K), whereas three components ($n=3$) are required to yield reasonable fits for the spectra above T_g. In such a situation, simultaneous fits of multiple spectra obtained under different longitudinal magnetic fields using a common set of parameters provide reliable results. One such set of data obtained at 30 K yields the result of curve fit shown in Fig. 9, with $\nu_1 = 1.48(18)\times 10^9$ s^{-1}, $\nu_2 = 1.72(34)\times 10^8$ s^{-1}, and $\nu_3 = 0.69(11)\times 10^7$ s^{-1} for a common Gaussian width of $\Delta_S = 19.3(5)$ MHz, all having comparable partial asymmetry. As shown in Fig. 10, these values of spin-fluctuation rate are spread over three orders of magnitude, clearly indicating that the spin dynamics of $Ca_2Ru_2O_7$ cannot be reduced to a simple model like Eq. (20) by assuming a unique correlation time ($\tau_c \equiv 1/\nu$) at a given temperature. The variation in T_g($\simeq$2–3 K) due to the mixture of two-batch samples appears to have a negligible influence on the temperature dependence of ν_i.

The nuclear dipolar width in $Ca_2Ru_2O_7$ [$\Delta = 0.128(2)$ MHz, determined from the spectra for $T \gg T_g$ without much ambiguity] is found to be considerably greater than that observed in $Hg_2Ru_2O_7$ and $Cd_2Ru_2O_7$, suggesting that the muon occupies a different site closer to Ru ions; ^{43}Ca is the only isotope of Ca nuclei with finite nuclear magnetic moments whose natural abundance is negligibly small (0.135%) and therefore is of no relevance to the change in Δ.

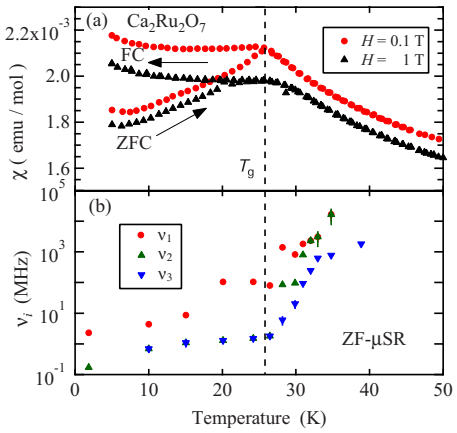

FIG. 10. (Color online) Temperature dependence of (a) bulk susceptibility (corresponding to one of the two-batch samples) and (b) fluctuation rate of the local fields probed by μSR in $Ca_2Ru_2O_7$. Three components with different fluctuation rates ($\nu_{1,2,3}$) are presumed in Eq. (18) for $T > T_g \simeq 25$ K and two of these ($\nu_{1,2}$) for $T < T_g$ (refer to text for details).

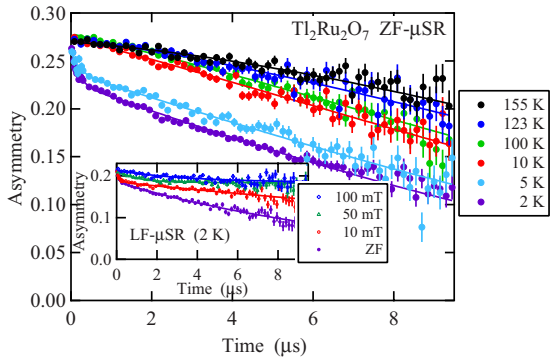

FIG. 11. (Color online) Time-dependent μ-e decay asymmetry observed in $Tl_2Ru_2O_7$ at various temperatures. Each spectrum is vertically shifted by 0.02 for clarity. Inset: the asymmetry observed at 2 K under a longitudinal field of 0, 10, 50, and 100 mT. Solid curves are the best fits obtained using Eq. (21).

However, considering that both nuclear and atomic dipolar moments are situated in the same Ru site, the magnitude of Δ_S is used to evaluate the effective atomic moment size of Ru ions from that of nuclear magnetic moments using Eqs. (9) and (17); the effective atomic moment size is evaluated to be 0.69(1) μ_B/Ru ($T < T_g$) or 0.35(1) μ_B/Ru($T > T_g$). The latter is in excellent agreement with the value estimated from the temperature dependence of bulk susceptibility obtained for single-crystalline specimen of $Ca_2Ru_2O_7$.[21]

It should be noted that the above-mentioned result clearly indicates a different origin of randomness in $Ca_2Ru_2O_7$ from that in the dilute alloy systems. This is clearly understood by considering the difference in the nature of the spin-spin interaction between these two cases. The RKKY interaction in the dilute alloys has a specific feature in that its sign randomly changes with the relative distance between the local moments located at random. Meanwhile, in the case of pyrochlore compounds, all the magnetic moments are located at the regular lattice positions; randomness is allowed only for the orientation of the moments. There is no obvious way of introducing randomness to the interaction between B-site ions. The description of the local field by Gaussian distribution in $Ca_2Ru_2O_7$ indicates the random orientation of Ru^{5+} local moments ($S=3/2$) as the primary source of the randomness, which might be phenomenologically described as a "frozen spin liquid" state.

D. $Tl_2Ru_2O_7$

Unlike the other three compounds, the Ru ions in $Tl_2Ru_2O_7$ are presumed to be tetravalent ($4d^4$), and therefore, one of the $4d$ electrons has orbital degeneracy in the t_{2g} manifold. Such a degenerate state is susceptible to the Jahn-Teller distortion that reduces free energy by breaking the local lattice symmetry, generally resulting in structural phase transition. In fact, $Tl_2Ru_2O_7$ is known to exhibit a clear structural transition at $T_s \simeq 120$ K in conjunction with the metal-insulator (or -semiconductor) transition; the reduction in symmetry from cubic-to-orthorhombic structure is found by means of powder neutron-diffraction studies.[18,19] The transition is also associated with a sharp decrease in magnetic susceptibility (χ) at T_s. The observed small hysteresis suggests that the reduction in χ might be due to the structural transition and associated opening of the band gap. These bulk properties are quite similar to those observed in $Hg_2Ru_2O_7$, leading to a naive speculation that the electronic ground state might be common for these two compounds.

However, it has been suggested from the Tl-NMR experiment that the ground state of $Tl_2Ru_2O_7$ is nonmagnetic and that it has an excitation gap (as inferred from the behavior of the spin-lattice relaxation rate, T_1^{-1}).[17] The recent inelastic neutron-scattering experiment also reports the occurrence of a well-defined excitation gap ($\simeq 11$ meV) below T_s.[19] The gap is attributed to the formation of one-dimensional Ru chains ($S=1$) along the [110] direction, which are believed to be a model system of Haldane chains.[19] Our μSR result supports the presence of a nonmagnetic ground state, and it provides further evidence for the formation of Haldane chains in this compound.

Figure 11 shows μSR time spectra under zero external field observed at various temperatures. They do not exhibit any anomaly in passing through $T_s \simeq 120$ K, and the line shape mostly indicates a slow Gaussian depolarization expected for random local fields arising from nuclear magnetic moments. (More specifically, the finite gradient $dA(t)/dt$ for $t \to 0$ indicates that an exponential damping due to paramagnetic fluctuation overlaps to the Gaussian damping; see below.) Thus, the result clearly demonstrates that the new ground state emerging below T_s does not accompany long-range magnetic order, as suggested by Tl-NMR. It should be noted that the line shape exhibits a gradual change from Gaussian to exponential damping with decreasing temperature and that a small fraction of the asymmetry shows rapid depolarization below $T^* \sim 10$ K. This quasistatic magnetism can be attributed to staggered moments at the open edges of Haldane chains;[27] these edges may be due to various crystalline defects including the twin boundaries inherent in the orthorhombic structure. A previous μSR study on another Haldane system (Y_2BaNiO_5, which has a similar gap energy)

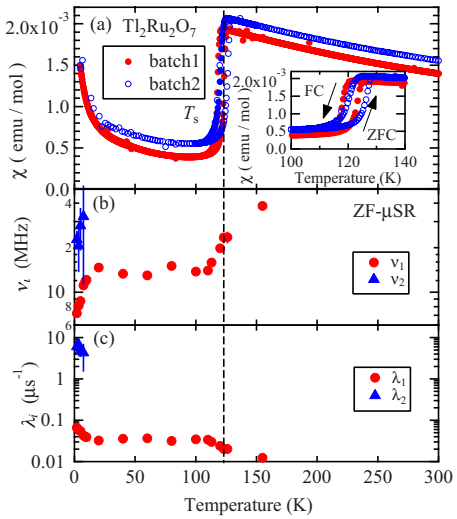

FIG. 12. (Color online) Temperature dependence of (a) bulk susceptibility (obtained from the respective batch of samples before mixing) and of fit parameters obtained by analysis using Eq. (21), namely, (b) fluctuation rate (ν_i), and (c) corresponding depolarization rate (λ_i) in $Tl_2Ru_2O_7$.

indicates that such staggered moments induce spin-glasslike random magnetism.[28]

Considering these features, we performed a curve-fitting analysis of the spectra using a simplified form of Eq. (16) with two components

$$A(t) \simeq G_z^{\mathrm{KT}}(t,\Delta)\sum_{i=1}^{2} A_i \exp(-\lambda_i t) + A_b, \tag{21}$$

$$\lambda_i = \frac{2\sigma_i^2, \nu_i}{\nu_i^2 + \gamma_\mu^2 H_0^2}, \quad (i = 1,2), \tag{22}$$

which is a good approximation in the paramagnetic state with $\nu_i \geq \sigma_i$. The hyperfine parameters (σ_i and Δ) are determined by the simultaneous fitting of multiple spectra obtained at 2 K under different longitudinal fields (H_0), yielding $\sigma_1 = 0.49(1)$ MHz, $\sigma_2 = 8.3(3)$ MHz, and $\Delta = 0.042(7)$ MHz. The value of Δ indicates that the muon site is common to that in $Hg_2Ru_2O_7$ and $Cd_2Ru_2O_7$. These values are fixed for the rest of the analysis extracting the spin-fluctuation rates (ν_i) from the curve fits for the ZF-μSR spectra; the result is shown in Fig. 12. The second component is observed only below T^* with A_2 showing a gradual increase with decreasing temperature ($\simeq 0.03$ at 2 K).

Interestingly, the fluctuation rate exhibits a gradual decrease as temperature is reduced toward T_s. This is in good agreement with the behavior of Tl-NMR T_1^{-1} interpreted as a manifestation of reduced spin excitation associated with the development of spin-singlet correlation. [The temperature dependence of ν_1 (and λ_1) near T_s is probably influenced by the variance of T_s($\simeq 5$ K) due to the mixture of two-batch samples, although the change is rather steep and is displayed in a logarithmic scale in Fig. 12.] The fact that ν_1 is levelled below T_s supports the view that μSR is also monitoring the same phenomenon through a different time window (i.e., it is not the artifact associated with muon diffusion).

A further slowdown of fluctuation (ν_1) is observed below T^*, where the second component attributed to the staggered moments appears with an intermediate fluctuation rate (ν_2). It is found that the emergence of this component occurs simultaneously with the appearance of a large Curie term in the magnetic susceptibility. Thus, the apparent "impurity"-like behavior in χ is explained by the edge states associated with the Haldane chains.

TABLE II. Effective Ru moment size in $A_2Ru_2O_7$ estimated from the magnitudes of local fields at muon site.

	T_m, T_g	Ru moment size
$Hg_2Ru_2O_7$	$\simeq 107$ K	0.5(1) μ_B
$Cd_2Ru_2O_7$	$\simeq 100$ K	0.36(7) μ_B
$Ca_2Ru_2O_7$	$T_g \simeq 25$ K	0.35(1) μ_B ($T > T_g$)
		0.69(1) μ_B ($T < T_g$)

IV. DISCUSSION

A. Correlation between magnetic randomness and itinerant character of 4*d* electrons

We have shown by μSR studies on a series of Ru pyrochlore compounds ($A_2Ru_2O_7$) that their electronic ground state exhibits a systematic change with the varying A cations. The change in the structural and MI transition temperature suggests that the relevant 4*d* electrons become more itinerant in the system with a less covalent A cation (Hg > Cd > Ca). This is also supported by the effective size of local Ru moments summarized in Table II, which tends to reduce along with the above-mentioned order (except below T_g in the case of $Ca_2Ru_2O_7$, where the moment appears to be restored on the suppression of spin fluctuation). While the effect of the variation in the covalency of AO sublattice on the RuO_6 network is not clear, the t_{2g} bandwidth ($\varepsilon_{d\epsilon}$) appears to be comparable to (or greater than) the energy gain caused by the local lattice distortion. It should be noted that the magnetism in the ground state exhibits a stronger randomness in the compounds showing more itinerant characteristics. The absence of structural change upon MI transition in $Cd_2Ru_2O_7$ might even suggest that the transition is of a Mott type ($U \geq \varepsilon_{d\epsilon}$ with U being the electronic correlation energy), as the t_{2g} band is half filled. The appearance of a more random magnetism at lower temperatures (below ~ 30 K) suggests that the magnetism just below $T_m \simeq 100$ K is not a fully fledged Néel state and that a significant amount of entropy is preserved. In this regard, it is worth noting that the Dzyaloshinski-Moriya (DM) interaction serves as a direct driving force for the secondary magnetic phase with an energy scale of 25–30 K (i.e., $\sim k_B T_{m2}$ in $Hg_2Ru_2O_7$ and $Cd_2Ru_2O_7$ and $\sim k_B T_g$ in $Ca_2Ru_2O_7$, which are close to each other, suggesting a common origin). The path of exchange interaction between Ru ions indeed lacks inversion symmetry; Ru ions are therefore subjected to the DM interaction that tends to rotate the Ru moments around the direction of

$\mathbf{S}_i \times \mathbf{S}_j$. This rotation along with the itinerant character of *d* electrons (see below) induces randomness in the electronic ground state of Ru pyrochlores.

According to the two-dimensional *t-J* model on a triangular lattice (in the vicinity of a half-filled band, where "*t*"$\sim\varepsilon_{d\epsilon}$ is the hopping integral and *J* is the Heisenberg exchange energy)[29,30] the presence of geometrical frustration leads to the competition in the ground state between Nagaoka ferromagnetism (which is rigorously proven for $J=0$ with one hole) and the Néel state for $t<0$; this, in turn, leads to a large degeneracy and the related entropy near $T=0$. The strong randomness in the magnetism observed in $Cd_2Ru_2O_7$ and $Ca_2Ru_2O_7$ might be due to a similar situation (with decreasing effective *J* in place of *t*) on the three-dimensional stage, where the quasistatic character of the local spins might imply a small effective *J* due to the two competing magnetic correlations.

B. Close similarity between $Ca_2Ru_2O_7$ and $Li_{1-x}Zn_xV_2O_4$

It has been found in previous studies that substitution of Li^+ with Zn^{2+} in LiV_2O_4 induces a spin-glass phase at low temperatures [for $x \geq 0.05$ in $Li_{1-x}Zn_xV_2O_4$, where the valence state of the vanadium is $V^{3.5-x/2}$ in the ionic limit].[31–33] This observation provides the experimental basis for the existence of geometrical frustration among vanadium ions, which also occupy the pyrochlore sublattice in the spinel structure. The compound exhibits metallic conductivity except at $x>0.9$ where a structural transition (cubic to tetragonal) occurs at a low temperature ($\simeq$50 K at $x=1$). Our detailed μSR study on $Li_{1-x}Zn_xV_2O_4$ has shown that the fluctuation of vanadium electronic moments ($\geq 10^9$ s^{-1}), which persists down to the lowest temperature in pure LiV_2O_4, is strongly suppressed below 4–5 K for $x=0.05-0.1$ and that a quasistatic random magnetism exists below $T_g \simeq 10$ K for $x \geq 0.2$.[9] The sensitivity of the V spin fluctuation to the slight variation in band filling suggests that the quater-filled state ($3d^{1.5}$ for $x=0$) in the vanadium t_{2g} band may be a "quantum critical point" (QCP) across the competing ground states.

Here, we point out that the result of μSR in $Ca_2Ru_2O_7$ shows a strong resemblance to that obtained in $Li_{1-x}Zn_xV_2O_4$. As shown in Fig. 13, the line shape of μSR spectra observed in the quasistatic spin-glass phase of $Li_{1-x}Zn_xV_2O_4$ with $x=0.2$ is well represented by the Kubo-Toyabe relaxation function (where the hyperfine parameter $\Delta_S \simeq 60$ MHz) with a small fraction ($\sim$20%) of the correction term [an exponential damping added to simulate Eq. (14) probably due to the randomness induced by the substitution of Li by Zn], indicating that the density distribution of local magnetic field probed by the muon is mostly represented by a Gaussian distribution.[34] This again suggests that the distribution is determined by the random orientation of V moments and that the origin of randomness is similar to that in the case of $Ca_2Ru_2O_7$. Considering that the spin-glass state is related to the heavy quasiparticle state in LiV_2O_4, the electronic ground state of $Ca_2Ru_2O_7$ might also be understood to be close to the QCP realized in LiV_2O_4.

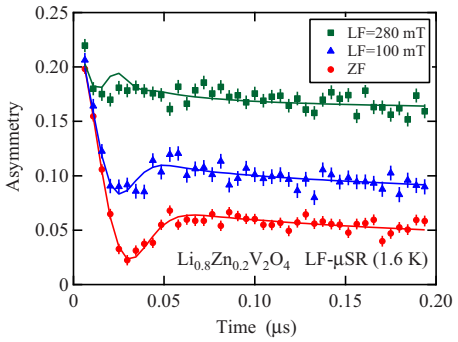

FIG. 13. (Color online) Time-dependent μ-*e* decay asymmetry observed in $Li_{1-x}Zn_xV_2O_4$ with $x=0.2$ at 1.6 K under a longitudinal field of 0, 10 mT, 0.1 T, and 0.28 T. Solid curves are the best fits obtained using Eq. (18) and a small fraction of the additive exponential damping term (refer to text for details).

V. CONCLUSIONS

We have shown by muon spin rotation study on a series of ruthenium pyrochlore oxides that the electronic ground state exhibits a systematic variation for different *A* cations and that the structural and metal-insulator transition temperature (T_s) is reduced with increasing covalency of the *A*O sublattice. The reduction in T_s and the enhanced itinerant character of the compounds is in accordance with the degree of randomness in the ground-state magnetism probed by μSR. The randomness arises from the random orientation of the ruthenium local magnetic moments. By means of a theoretical investigation using the two-dimensional *t-J* model on a triangular lattice, we indicate that the origin of such a "spin-orientarion glass" state may be due to the competition between the Nagaoka ferromagnetic correlation and the antiferromagnetic exchange interaction in the vicinity of the Mott-insulating phase (for the half-filled t_{2g} bands); this interaction occurs in conjunction with the local Dzyaloshinski-Moriya interaction.

ACKNOWLEDGMENTS

We would like to thank the TRIUMF staff for their technical support during the μSR experiment and also thank Masao Ogata for the helpful discussion. This work was partially supported by the KEK-MSL Inter-University Research Program for Overseas Muon Facilities and by a Grant-in-Aid for Creative Scientific Research on Priority Areas from the Ministry of Education, Culture, Sports, Science and Technology, Japan.

[1] J. Pannetier and J. Lucas, Mater. Res. Bull. **5**, 797 (1970).
[2] S. R. Dunsiger, R. F. Kiefl, K. H. Chow, B. D. Gaulin, M. J. P. Gingras, J. E. Greedan, A. Keren, K. Kojima, G. M. Luke, W. A. MacFarlane, N. P. Raju, J. E. Sonier, Y. J. Uemura, and W. D. Wu, Phys. Rev. B **54**, 9019 (1996).
[3] J. S. Gardner, B. D. Gaulin, S. H. Lee, C. Broholm, N. P. Raju, and J. E. Greedan, Phys. Rev. Lett. **83**, 211 (1999).
[4] M. J. Harris, S. T. Bramwell, D. F. McMorrow, T. Zeiske, and K. W. Godfrey, Phys. Rev. Lett. **79**, 2554 (1997).
[5] A. P. Ramirez, A. Hayashi, R. J. Cava, R. Siddharthan, and B. S. Shastry, Nature (London) **399**, 333 (1999).
[6] Y. Taguchi and Y. Tokura, Phys. Rev. B **60**, 10280 (1999).
[7] T. Katsufuji, H. Y. Hwang, and S.-W. Cheong, Phys. Rev. Lett. **84**, 1998 (2000).
[8] S. Kondo, D. C. Johnston, C. A. Swenson, F. Borsa, A. V. Mahajan, L. L. Miller, T. Gu, A. I. Goldman, M. B. Maple, D. A. Gajewski, E. J. Freeman, N. R. Dilley, R. P. Dickey, J. Merrin, K. Kojima, G. M. Luke, Y. J. Uemura, O. Chmaissem, and J. D. Jorgensen, Phys. Rev. Lett. **78**, 3729 (1997).
[9] A. Koda, R. Kadono, W. Higemoto, K. Ohishi, H. Ueda, C. Urano, S. Kondo, M. Nohara, and H. Takagi, Phys. Rev. B **69**, 012402 (2004).
[10] A. Koda, R. Kadono, K. Ohishi, S. R. Saha, W. Higemoto, Y. Matsushita, and Y. Ueda, J. Phys.: Condens. Matter **17**, L257 (2005).
[11] M. Shiga, K. Fujisawa, and H. Wada, J. Phys. Soc. Jpn. **62**, 1329 (1993).
[12] J. Reading, S. Gordeev, and M. T. Weller, J. Mater. Chem. **12**, 646 (2002).
[13] D. Mandrus, J. R. Thompson, R. Gaal, L. Forro, J. C. Bryan, B. C. Chakoumakos, L. M. Woods, B. C. Sales, R. S. Fishman, and V. Keppens, Phys. Rev. B **63**, 195104 (2001).
[14] R. Wang and A. W. Sleight, Mater. Res. Bull. **33**, 1005 (1998).
[15] A. Koda, K. H. Satoh, R. Kadono, S. Yonezawa, Y. Muraoka, and Z. Hiroi (unpublished).
[16] A. Koda, R. Kadono, K. Ohishi, S. R. Saha, W. Higemoto, S. Yonezawa, Y. Muraoka, and Z. Hiroi, J. Phys. Soc. Jpn. **76**, 063703 (2007).
[17] H. Sakai, M. Kato, K. Yoshimura, and K. Kosuge, J. Phys. Soc. Jpn. **71**, 422 (2002).
[18] T. Takeda, R. Kanno, Y. Kawamoto, M. Takano, F. Izumi, A. W. Sleightd, and A. W. Hewate, J. Mater. Chem. **9**, 215 (1999).
[19] S. Lee, J.-G. Park, D. T. Adroja, D. Khomskii, S. Streltsov, K. A. McEwen, H. Sakai, K. Yoshimura, V. I. Anisimov, D. Mori, R. Kanno, and R. Ibberson, Nature Mater. **5**, 471 (2006).
[20] A. Yamamoto, P. A. Sharma, Y. Okamoto, A. Nakao, H. A. Katori, S. Niitaka, D. Hashizume, and H. Takagi, J. Phys. Soc. Jpn. **76**, 043703 (2007).
[21] T. Munenaka and H. Sato, J. Phys. Soc. Jpn. **75**, 103801 (2006).
[22] R. S. Hayano, Y. J. Uemura, J. Imazato, N. Nishida, T. Yamazaki, and R. Kubo, Phys. Rev. B **20**, 850 (1979).
[23] M. Yoshida, M. Takigawa, A. Yamamoto, and H. Takagi (unpublished).
[24] R. E. Walstedt and L. R. Walker, Phys. Rev. B **9**, 4857 (1974).
[25] C. Held and M. W. Klein, Phys. Rev. Lett. **35**, 1783 (1975).
[26] K. W. Kehr, G. Honig, and D. Richter, Z. Phys. B **32**, 49 (1978).
[27] M. Hagiwara, K. Katsumata, I. Affleck, B. I. Halperin, and J. P. Renard, Phys. Rev. Lett. **65**, 3181 (1990).
[28] K. Kojima, A. Keren, L. P. Le, G. M. Luke, B. Nachumi, W. D. Wu, Y. J. Uemura, K. Kiyono, S. Miyasaka, H. Takagi, and S. Uchida, Phys. Rev. Lett. **74**, 3471 (1995).
[29] T. Koretsune and M. Ogata, Phys. Rev. Lett. **89**, 116401 (2002).
[30] T. Koretsune and M. Ogata, J. Phys. Soc. Jpn. **72**, 2437 (2003).
[31] Y. Ueda, N. Fujiwara, and H. Yasuoka, J. Phys. Soc. Jpn. **66**, 778 (1997).
[32] W. Trinkl, N. Büttgen, H. Kaps, A. Loidl, M. Klemm, and S. Horn, Phys. Rev. B **62**, 1793 (2000).
[33] A. Krimmel, A. Loidl, M. Klemm, S. Horn, and H. Schober, Physica B **281–282**, 26 (2000).
[34] A. Koda, R. Kadono, W. Higemoto, K. Ohishi, H. Ueda, C. Urano, S. Kondo, M. Nohara, and H. Takagi (unpublished).